JOURNAL OF MATERIALS SCIENCE 8 (1973) 571–576

Grain-boundary energy of copper at 1030°C

M. McLEAN
Division of Inorganic and Metallic Structure, National Physical Laboratory, Teddington, Middlesex, UK

The grain-boundary energies of individual boundaries have been determined by the analysis of the shapes of grain-boundary grooves. The effects of surface-energy anisotropy are fully taken into account. The results indicate that only boundaries associated with high-coincidence orientations ($\sum 3$ and $\sum 11$) have significantly lower energies than average high-angle grain boundaries.

1. Introduction

Although dislocation theory has provided satisfactory models for low-angle tilt and twist boundaries, there is still considerable debate concerning the structure of large-angle grain boundaries. Brandon *et al* [1] generalized the coincidence-lattice model of Hargreaves and Hills [2] which attributes special properties to the boundaries between crystals which are oriented so that a fraction of the lattice sites of each crystal coincides. The degree of coherency associated with such boundaries is completely destroyed by even very small deviations from the coincidence orientation. Other authors [3] have suggested that coincidence in the boundary plane can be attained even when the crystals do not have a coincidence relationship. Brandon [4] and Bollmann [5] have proposed that boundary coincidence, between crystals which deviate slightly from a coincidence misorientation (by $< 10°$), can be achieved by the superposition of a regular array of dislocations, or steps, on the simple coincidence-lattice boundary.

Experimental evidence relating to grain-boundary structure is meagre. The lateral resolution of available microscopical techniques, including field-ion and electron microscopy, are inadequate to resolve details of grain-boundary structure. However, dislocations in, or near, grain boundaries have been observed, by both field-ion [6] and electron microscopy [7], and the Burgers vectors of some of them have been demonstrated to bear no simple relationship to either crystal lattice, suggesting that they are indeed associated with the boundary rather than either crystal lattice.

Indirect evidence is available from a number of sources. For example, Aust and Rutter [8] have observed that boundaries between coincidence-oriented crystals are considerably more mobile than random high-angle grain boundaries. Similarly data from grain-boundary sliding experiments [9] show considerable crystallographic anisotropy which correlates with known coincidence misorientations.

Any grain-boundary structure should be reflected in the anisotropy of grain-boundary energy, σ. However, unambiguous quantitative measurement of σ is difficult. Moreover, a systematic study of σ in terms of the five parameters necessary to define the orientation of a given grain boundary would be extremely complex. In the course of experiments to determine surface-energy anisotropies [13], we have accumulated results for the grain-boundary energies of some well-defined high-angle boundaries. These data will be presented below, and their significance to the coincidence site model noted.

It is convenient to consider two aspects of the anisotropy of grain-boundary energy. First, the effect of varying the boundary orientation between crystals of fixed misorientation is completely analogous to surface energy anisotropy. More important however, for grain boundaries is the variation in grain-boundary energy with crystal misorientation. We shall discuss the results in terms of each of these effects.

2. Data analysis

The equilibrium configuration of the groove formed at the intersection of three interfaces is completely determined by the free energies of the interfaces. Several studies of variations of grain-boundary energy with crystallographic orientation have involved the careful examination of (i) grooves formed at the intersection of a grain boundary with a crystal surface [10], or (ii) the configuration at the junction of three grain boundaries [11]. An approximate form of the equilibrium equation has commonly been used to determine the *mean* value of σ.

$$\sigma = 2\gamma \cos \theta \qquad (1)$$

where γ is the *mean* value of the surface energy and 2θ is the dihedral angle.

Herring [12] has derived a more complete condition for equilibrium in crystalline materials where both σ and γ may vary with orientation.

$$\sigma = \gamma(\mathbf{n}_1) \cos \theta_1 + \gamma(\mathbf{n}_2) \cos \theta_2 + \frac{\partial \gamma(\mathbf{n}_1)}{\partial \theta} \sin \theta_1 + \frac{\partial \gamma(\mathbf{n}_2)}{\partial \theta} \sin \theta_2 \qquad (2)$$

where $\mathbf{n}_1$, $\mathbf{n}_2$ are unit vectors normal to the crystal surfaces at the groove roots and θ_1, θ_2 are dihedral angles defined in Fig. 1. If it is desired to determine variations of σ, it is inconsistent to use Equation 1, which assumes that both σ and γ are isotropic. Several authors [10, 11] have argued that, since $\partial\gamma/\partial\theta \ll \gamma$, use of Equation 1 introduces a negligible error. However, the magnitude of the error involved in such simplification may be demonstrated as follows:

Consider the typical case where $\theta_1 = \theta_2 = 80°$,

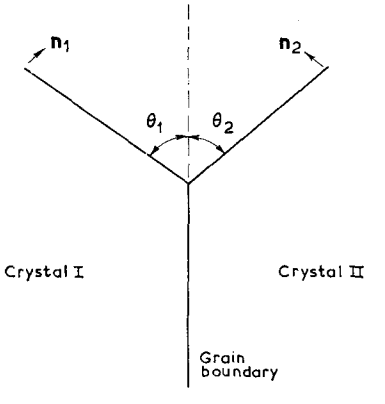

Figure 1 A schematic section of a grain-boundary groove defining the dihedral angles θ_1 and θ_2

and let us assume extremely low surface-energy anisotropy. For the case of clean copper at 1030°C, a 1.7% variation of γ can give rise to maximum surface-torque terms, $1/\gamma(\partial\gamma/\partial\theta)$, of 0.1 rad^{-1} [13]. Let us consider the uncertainty in determining σ from the groove profile due to a torque of 0.05 rad^{-1} (which may be either positive or negative).

From Equation 1 $\sigma/\gamma = 0.35$

Equation 2 $= 0.35 \pm 0.10$.

Thus a surface energy anisotropy of about 1% can give rise to a 30% error in the measurement of σ, and this may be erroneously attributed to a 30% anisotropy of σ. Similarly we may show that at the intersection of three grain boundaries (where $\theta_1 = \theta_2 \sim 60°$), the torque terms due to a 1% grain-boundary anisotropy may introduce a 10% scatter on results derived from Equation 1. A corollary of this argument is that an approximate analysis of grain-boundary equilibrium angles, neglecting torques, will always considerably overestimate the real anisotropy of grain-boundary energy. Thus, continuing the above illustration, a $77\frac{1}{2}$ to $82\frac{1}{2}°$ range of dihedral angles would, from Equation 1, suggest a 25% anisotropy of σ. However, the same variation could be wholly attributed to a 0.05 rad^{-1} surface torque (or 1% surface energy anisotropy) and zero anisotropy of σ.

3. Experimental measurements

We have adopted two approaches to the analysis of grain-boundary groove profiles in order to fully compensate for surface-energy anisotropy and hence yield a true estimate of grain-boundary energies of specific well-defined grain boundaries.

3.1. Wire specimens

When a fine wire is annealed at high temperature a "bamboo structure" often develops, i.e., grain boundaries extend through and normal to the axis of the wire. Careful analysis of changes of groove shape around the perimeter of the wire has provided a method of measuring surface-energy anisotropies [13]. In addition the analysis provides the grain-boundary energy, *fully corrected for surface torques*, of isolated grain boundaries of known orientation.

The technique has been fully described in the literature. Surface energy anisotropy is represented by an analytical expression of finite order, say a double Fourier series. On substitution, Equation 2 becomes a linear equation with the coefficients of the surface-energy representation

and the grain-boundary energy as unknowns. If sufficient experimental data are available, dependent on the order of the representation, the set of linear equations can be solved by standard computer techniques.

In practice some sixty to eighty measurements are made on each grain boundary as the wire is systematically rotated. No control over the production of specific grain boundaries is possible so that systematic measurements as a function of boundary orientation are not possible. Nevertheless, valuable information on grain-boundary energies, somewhat randomly collected, can be compiled.

3.2. Sheet specimens

A well-annealed thin metal sheet is normally composed of a series of grains extending through the sheet with grain boundaries normal to the sheet. The grain-boundary groove profiles can be reconstructed using interference microscopy and, if the γ-plot has already been determined by the technique described above, the grain-boundary energy can be computed using Equation 2.

This approach has been adopted to determine the energies associated with incoherent twin boundaries. The analysis is described in the Appendix and depends on the assumption that the boundary is normal to the surfaces of the sheet and can only be applied to incoherent twin boundaries whose traces on the surface are normal to the matching coherent twin-boundary trace.

The misorientation of twinned crystals is well defined and fixed. Consequently the only anisotropy of twin-boundary energy is associated with the inclination of the boundary plane with respect to the twinning plane. This anisotropy can therefore be represented, as is the γ-plot, by a polar plot of σ_T*. This experiment will only give information concerning those incoherent boundaries whose surface normals make a right angle with the normal to the twinning plane.

4. Experimental

High-purity copper wire, of 0.13 mm diameter, was annealed in dry hydrogen for 2 h at 1030° C. The grain-boundary groove profiles were examined by electron microscopy, using a specimen holder capable of rotating the specimen in the electron beam about the wire axis (Fig. 2). The grain-boundary orientations were established using standard Laue X-ray back-reflection techniques. These data were analysed using a KDF9 computer programmed in Algol.

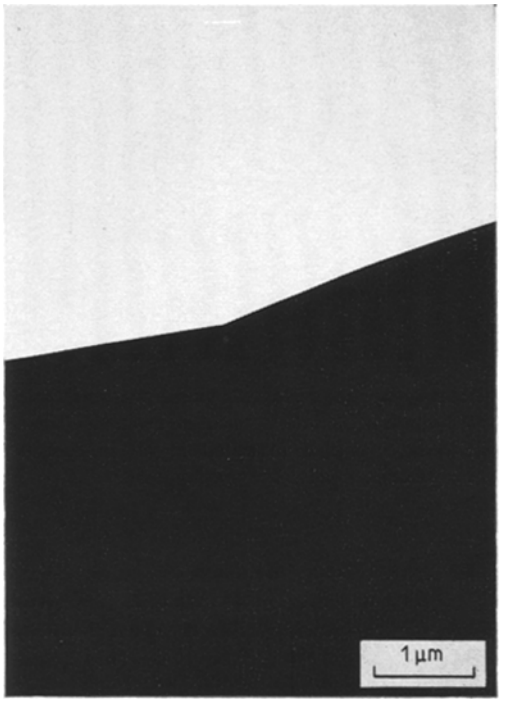

Figure 2 A typical electron shadowgraph of a grain-boundary groove in copper annealed in dry hydrogen at 1030° C.

Similar material in sheet form was prepared and was annealed in closely parallel conditions. The groove profiles were examined by interference microscopy (Fig. 3) and the crystal orientations determined by a twin-trace technique.

5. Results

A summary of the grain-boundary energies of copper at 1030° C in dry hydrogen (dew point = − 70° C) is shown in Fig. 4 in the form of a histogram of the ratio of grain-boundary energy to the surface energy of a (100) crystal surface. This has been computed using experimental results for surface-energy anisotropy obtained by analysis of these data [13].

Of some twenty high-angle grain boundaries which were fully analysed using wire specimens, only one was found to separate crystals with a high coincidence misorientation. The non-coincidence boundaries showed no significant variation of grain-boundary energy, $\sigma/\gamma_{100} = 0.32 \pm 0.01$. However, one boundary, separating

*The radius vector is proportional in length to the magnitude of σ_T and parallel to the normal to the boundary.

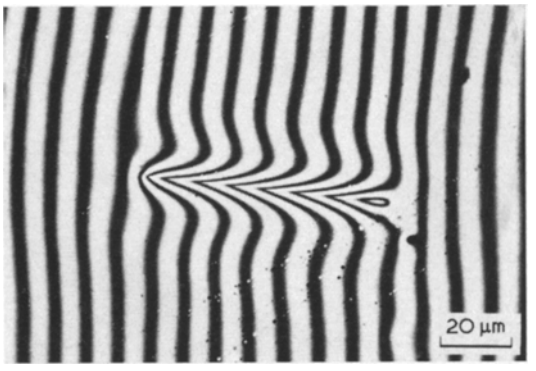

Figure 3 A typical interferogram of the groove formed at the intersection of an incoherent twin boundary with the crystal surface, copper annealed in dry hydrogen at 1030° C. (Thallium light, $\lambda/2 = 0.26$ μm.)

crystals which were misoriented by a 50° 30′ (± 1°) rotation about a [1 1 0] axis, was found to have a considerably lower grain-boundary energy: $\sigma/\gamma_{100} = 0.26 \pm 0.01$. The orientation of this boundary is shown in Fig. 5.

No significant variation of incoherent twin-boundary energy with boundary inclination was detected: $\sigma/\gamma_{100} = 0.21 \pm 0.01$. This suggests that the σ_T plot is circular in section normal to the axis of the twinning plane. However, the boundary energy between twinned crystals (i.e., [1 1 0] 70°30′ rotation) is some 30% lower than general high-angle boundary energies.

6. Discussion

Under the experimental conditions described there is little variation of high-angle grain-boundary energy. However, boundaries separating crystals of high coincidence ($\sum = 3$ and $\sum = 11$)* have significantly lower energy such that

$$\sigma_{(\Sigma=3)} < \sigma_{(\Sigma=11)} < \sigma_{av}.$$

This is the order one might expect from considerations of the coherency of the boundaries. Since $\sum = 3$ and 11 boundaries have roughly 33 and 9% coherencies respectively, one might expect the decreases of grain-boundary energy to be of similar magnitude. Experimentally we find decreases of 33 and 20% respectively.

No control was exercised over the misorientation of adjacent crystals. Consequently no information is available concerning the high-coincidence $\sum = 5$, 7 and 9 boundaries, since they did not occur naturally in the specimens examined. Theoretically the energies of such boundaries would be expected to be intermediate between $\sigma_{(\Sigma=3)}$ and $\sigma_{(\Sigma=11)}$.

The measurements of incoherent twin-boundary energy suggest that, at high temperature, there is little dependence on boundary inclination for fixed crystal misorientation. Indeed our results indicate that the σ_T plot is generally spherical with a sharp cusp at the coherent twin-boundary orientation

$$(\sigma_{coherent}/\gamma_{100} = 0.02).$$

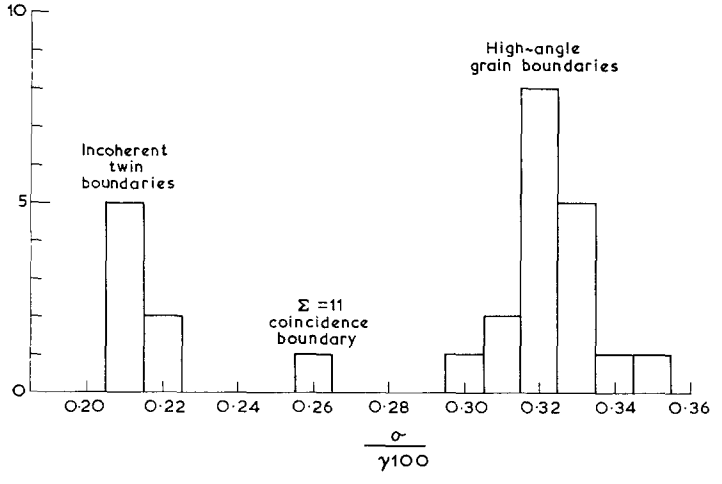

Figure 4 Histogram of the ratio of grain-boundary energy (σ) to the surface energy of (100) (γ_{100}) for copper annealed in dry hydrogen at 1030° C.

*In this nomenclature, Σ is the reciprocal of the relative density of coincidence sites. Thus in the fcc lattice, $\Sigma=3$ for twinned crystals and $\Sigma=11$ for 50°30′ [1 1 0] oriented crystals.

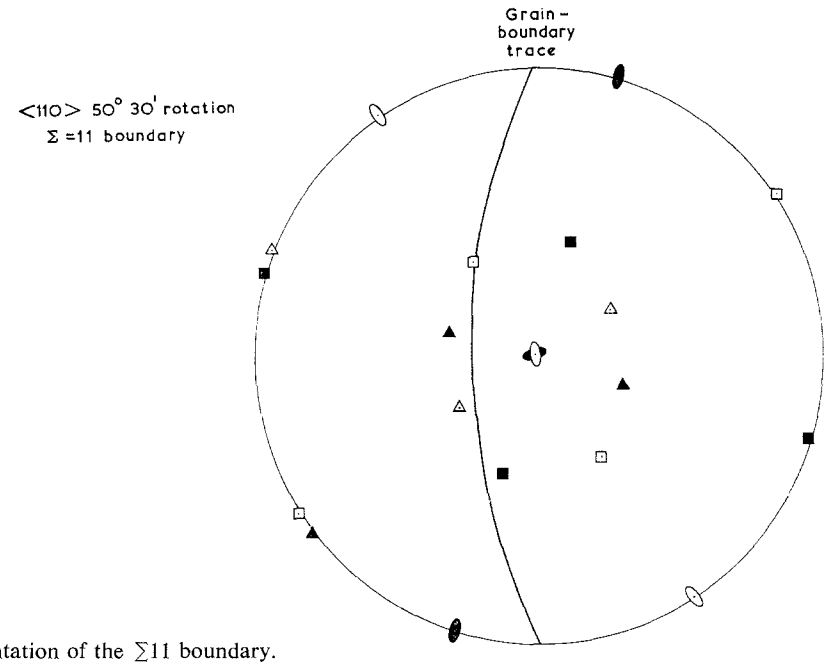

Figure 5 Orientation of the $\sum 11$ boundary.

The experimental results do not show the large number of cusps predicted by various calculations of grain-boundary energies as a function of crystal misorientation. At best we can say that, with the exception of $\sum = 3$ and $\sum = 11$ boundaries, the anisotropy of grain-boundary energy is less than 10%. This is considerably less than the predicted anisotropy. However, the computations do not include any assessment of either configurational or vibrational entropy and hence strictly refer only to 0 K.

A more phenomenological approach might be to consider an arbitrary grain boundary as a superposition of a neighbouring coincidence boundary and an array of dislocations. The dislocation array would be that which yields the required misorientation with the least total dislocation energy. A measure of the depth of a given grain-boundary cusp may be obtained from an estimate of the energy and entropy of the dislocation array. Ishida and McLean [14] have shown that the Burgers vectors of the dislocations associated with such arrays are considerably smaller than those of lattice dislocations. Indeed the magnitude of the allowed Burgers vectors tend to be smallest for boundaries of low coincidence, they vary with $\sum^{-\frac{1}{2}}$. Consequently the depth of cusps associated with coincidence boundaries will, on this model, be related to the extent of boundary coincidence. The energy associated with the dislocation array may be obtained using the familiar expression for the energy of a low-angle boundary but allowing the Burgers vectors to be those associated with grain-boundary dislocations. Thus

$$\triangle\sigma = \tfrac{1}{2}\mu\, \boldsymbol{b}\, \theta\, (\mathrm{A} - \ln \theta)$$

where μ, A are constants, θ is the deviation from coincidence and $\triangle\sigma = \sigma_\theta - \sigma_{\text{coincidence}}$.

This would predict that $\triangle\sigma_{\Sigma 3}{:}\triangle\sigma_{\Sigma 11} = 1.9$ which compares with our experimentally determined value of 1.8. This agreement is probably fortuitous; however, it does provide a qualitative understanding of the blunting and eventual disappearance of the more minor cusps due to the entropy associated with dislocation arrrays in off-coincidence boundaries.

Acknowledgements

The author would like to thank G. Verney for experimental assistance and E. D. Hondros, D. McLean and H. Mykura for comments on this paper.

Appendix

Consider an incoherent twin boundary in a thin sheet of metal and assume the boundary is normal to the sheet (Fig. A1). $\mathbf{e}_1$ is a unit vector normal to the crystal surface; $\mathbf{n}_1$, $\mathbf{n}_2$ are normals to the surfaces at the pit of the grooves; $\mathbf{e}_3$ is normal to the boundary. The normal to the groove surface $\mathbf{n}$ can then be written

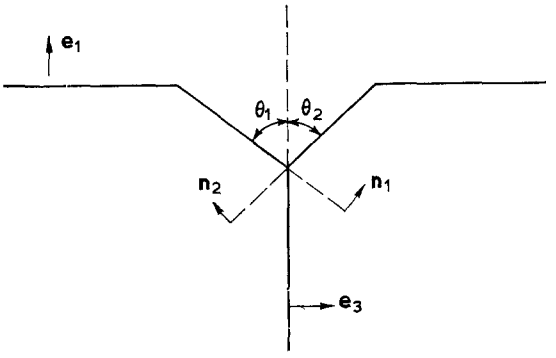

Figure A1 Schematic profile of a grain-boundary groove defining the various vectors used in the analysis.

$$\mathbf{n} = \sum_{i=1}^{3} n_i \, \mathbf{e}_i$$

where $n_1 = \sin\chi$, $n_2 = 0$, $n_3 = \cos\chi$; χ is the dihedral angle such that $\mathbf{e}_3 \cdot \mathbf{n} = \cos\chi$. Alternatively $\mathbf{n}$ may be referred to the cubic axes of the crystal $\mathbf{a}_i$.

$$\mathbf{n} = \sum_{i=1}^{3} Z_i \, \mathbf{a}_i$$

As shown previously [13], the coefficients n_i, Z_i can be related by the Euler matrix **E**. Indeed the analysis described in the appendix of reference 13, remains valid with $\beta = 0$. Having previously derived an expression for the anisotropy of surface energy

$$\gamma(\theta, \phi) = \sum_{m=-R}^{R} \sum_{n=-R}^{R} P_{mn} \exp[\mathrm{i}(2m\theta + n\phi)] ,$$

the experimentally determined values of P_{mn} can be substituted in Equation A15 of reference 13 to yield the grain-boundary energy of the incoherent twin boundary under consideration, fully corrected for surface-energy anisotropy.

By inspection of Fig. A2 the orientation of the incoherent twin boundary can be completely specified by two angular parameters α, β and by symmetry only $0 \geqslant \beta \geqslant 30°$ need be considered. In our particular experimental procedure, the normal to the incoherent boundary, $\mathbf{e}_3$, is at right angles to the normal to the twinning plane $\mathbf{t} = (l_1 \mathbf{a}_1 + l_2 \mathbf{a}_2 + l_3 \mathbf{a}_3)\sqrt{3}$ where the l_1's have the values + 1 or − 1, i.e.,

$$\mathbf{t} \cdot \mathbf{e}_3 = 0 .$$

Define a set of axes $\mathbf{A}_1 = \mathbf{t}$, $\mathbf{A}_2 = \mathbf{A}_1 \times \mathbf{a}_1$, $\mathbf{A}_3 = \mathbf{A}_1 \times \mathbf{A}_2$, then

$$\tan\beta = \frac{\mathbf{e}_3 \cdot \mathbf{A}_3}{\mathbf{e}_3 \cdot \mathbf{A}_2} = \frac{3 \cos\alpha_2 \sin\alpha_3}{l_3 \sin\alpha_2 \sin\alpha_3 - l_2 \cos\alpha_3}$$

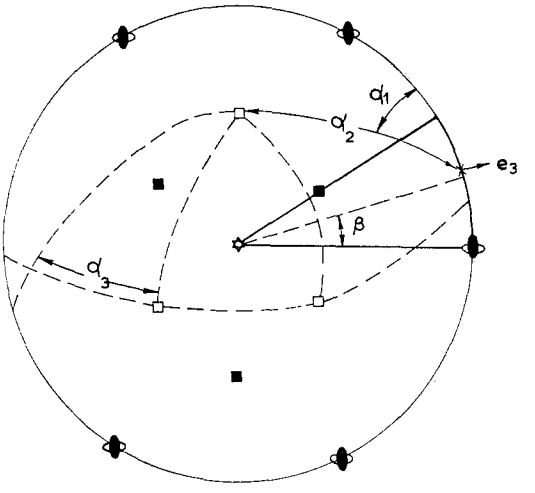

Figure A2 Stereogram defining the various axes and Euler angles described in the Appendix.

where α_1, α_2, α_3 are the Eulers angles defined in Fig. A2.

If the surface energy coefficients P_{mn} are known from previous experimentation, analysis of each data set of grain-boundary dihedral angles and crystallographic orientation (α_1, α_2, α_3) yields the fully corrected boundary energy as a function of β.

References

1. D. G. BRANDON, B. RALPH, S. RANGANATHAN, and M. S. WALD, *Acta Metallurgica* **12** (1964) 813.
2. F. HARGREAVES and R. J. HILLS, *J. Inst. Metals* **41** (1929) 257.
3. G. BISHOP and B. CHALMERS, *Scripta Met.* **2** (1968) 133.
4. D. G. BRANDON, *Acta Metallurgica* **14** (1966) 1479.
5. W. BOLLMANN, *Phil. Mag.* **16** (1967) 383.
6. B. LOBERG and H. NORDEN, *Arkiv för Fysik* **40** (1970) 413.
7. T. SCHOBER and R. W. BALLUFFI, *Phil. Mag.* **21** (1970) 109.
8. J. RUTTER and K. T. AUST, *Acta Metallurgica* **13** (1966) 181.
9. M. BISCONDI and C. GOUX, *Mem. Sci. Rev. Métall.* **65** (1968) 167.
10. K. T. AUST. in "Surfaces and Interfaces I", ed. J. E. Burke, N. L. Reed, and V. Weiss (Syracuse University Press, Syracuse, 1968).
11. H. GLEITER, *Acta Metallurgica* **18** (1970) 23; M. HASSON and C. GOUX, *Compt. Rend. Acad. Sci. Paris* **273C** (1971) 649.
12. C. HERRING, "Physics of Powder Metallurgy" ed. W. E. Kingston (McGraw-Hill, New York, 1951).
13. M. MCLEAN and B. GALE, *Phil. Mag.* **20** (1969) 1033,
14. Y. ISHIDA, and M. MCLEAN, *ibid*, in press.

Received 11 August and accepted 7 October 1972.